

Proof-of-concept demonstration of the PEGASES plasma thruster

*Presented at Joint Conference of 30th International Symposium on Space Technology and Science,
34th International Electric Propulsion Conference and 6th Nano-satellite Symposium
Hyogo-Kobe, Japan
July 4–10, 2015*

Trevor Alain Lafleur*
*Ecole Polytechnique, Palaiseau, 91128, France
ONERA - The French Aerospace Lab, Palaiseau, 91120, France*

Dmytro Rafalskyi†, Pascal Chabert‡ and Ane Aanesland§
Ecole Polytechnique, Palaiseau, 91128, France

Here we experimentally demonstrate the working principle of a gridded plasma thruster that alternatively extracts and accelerates both positive and negative ions to generate thrust. The plasma is created in an inductively coupled plasma source, and negative ion formation is enhanced by cooling electrons using a magnetic filter, which creates an almost electron-free plasma region near the source exit. By then applying square voltage waveforms with frequencies between 20-950 kHz, positive and negative ions are extracted and accelerated to high energies (100's of eV). Downstream measurements show that at sufficiently large frequencies the ion beams can be well neutralized. The behaviour of the measured ion current with frequency is explained with an analytical model which extends the Child-Langmuir law to AC ion acceleration.

Nomenclature

\mathbf{B}	= Magnetic field
\mathbf{E}	= Electric field
f	= Square waveform frequency
J^{dc}	= Net dc ion current density
J^{ac}	= Time-averaged ac ion current density
J^{CL}	= Space-charge limited current density
L	= Grid gap length
M	= Ion mass
n	= Subscript: negative ions
p	= Subscript: positive ions
q	= Ion charge
V_0	= Square waveform amplitude
α	= Square waveform duty cycle
ϵ_0	= Permittivity of free space

*Postdoctoral research fellow, Laboratoire de Physique des Plasmas, trevor.lafleur@lpp.polytechnique.fr

†Postdoctoral research fellow, Laboratoire de Physique des Plasmas, dmytro.rafalskyi@lpp.polytechnique.fr

‡Director, Laboratoire de Physique des Plasmas, pascal.chabert@lpp.polytechnique.fr

§Research group leader, Laboratoire de Physique des Plasmas, ane.aanesland@lpp.polytechnique.fr

I. Introduction

Gridded ion thrusters represent some of the earliest and most successful electric propulsion systems to date, due in large part to the high specific impulses that can be achieved, and their excellent power efficiencies.¹ In their simplest form these thrusters consist of a source cavity where a plasma is produced (using a number of different mechanisms including, microwave, rf, or dc hollow cathode discharges), and a set of grids to which a high voltage is applied (typically 100's to 1000's of volts depending on the propellant gas used). Positive ions are then extracted and accelerated to high energy, and beam stalling is prevented and neutralization² achieved by using a hollow cathode electron source external to the plasma source.¹ Thus the downstream quasi-neutral plasma consists of both positive ions and electrons.

In addition to the grids, the hollow cathode neutralizer represents one of the most life-limiting components of current electric propulsion systems. Operation of hollow cathodes can also be very sensitive to surface/propellant gas contamination, and they require an additional propellant gas supply line, as well as additional power supplies. Because of problems with scaling down these hollow cathodes, for many small ion thrusters the hollow cathode is usually a similar or larger size than the actual plasma source itself.³

There are a number of possible future space missions where having large numbers of electrons in the downstream plasma plume could present a distinct problem. For example, the removal of space debris⁴ has started to receive increased attention in the community due to the exponentially increasing amount in low Earth orbits. A number of different proposals, such as the LEOSWEEP project,⁴ have been made to try and reduce this debris using special "Shepherd" spacecraft which would fire a directed ion beam at the target debris, and force it into a lower orbit where it would eventually burn up in the Earth's atmosphere. These proposals typically involve the "Shepherd" spacecraft to be of the order of 10's to 100's of meters away, which requires a very low divergence ion beam. However, due to the presence of the Earth's magnetic field there are concerns that thrusters with electrons in the plasma plume will be significantly deflected over such distances, and hence increase the beam divergence.

A new thruster was proposed some years ago that can possibly meet these requirements.⁵ PEGASES (Plasma propulsion using Electronegative GASES) makes use of an electronegative gas in an rf plasma source, and produces both positive and negative ions which are then alternatively extracted and accelerated to generate thrust. The alternate acceleration scheme, when applied at large enough frequencies, allows the individually charged ion beam packets to mutually neutralize in the downstream exhaust plume; thus removing the need for an electron hollow cathode neutralizer. This concept has recently been experimentally demonstrated,⁶ and here we review some of these experimental⁶⁻⁸ and theoretical⁹ efforts.

II. Experimental apparatus

A schematic of the PEGASES plasma thruster is shown in Fig. 1. The plasma source is a rectangular aluminium box with a length of 12 cm, a width of 12 cm, and a height of 8 cm. The source is terminated at one end by a 2 mm thick ceramic window, and at the opposite end by a set of two stainless steel grids. In direct contact with the ceramic window is a 7-turn rf antenna embedded in ferrite (Ferroxcube 4C65). The grids are separated by a distance of 2 mm, and are each 1 mm thick with a transparency of about 60%, and an aperture diameter of 2.5 mm. The antenna is connected to a rf matching network consisting of a transmission line transformer and two variable capacitors, as well as a power meter and an rf power generator (operated at 4 MHz). A set of two neodymium bar magnets (known as a magnetic filter¹⁰) are placed on the top and bottom of the source (external to the plasma) about 7.5 cm from the ceramic backwall, and which give a maximum field strength of about 245 G.

Placed inside the aluminium plasma source is a smaller rectangular Pyrex tube. Along two opposite sides of the Pyrex tube are a row of 8 holes which serve as the injection location for the input gas. In the present proof-of-concept demonstration, sulphur hexafluoride (SF₆) is used, because of its highly electronegative nature, its low cost and ease of availability, and because it is well used and understood in industry. Connected to the grids is a PG2-500 single-phase inverter which generates the square voltage waveforms. The second downstream grid is grounded. The PEGASES plasma source is connected to a larger vacuum chamber with a diameter of 60 cm and a length of about 70 cm. This vacuum chamber is pumped down with a combination of rotary and turbomolecular pumps, and the base pressure is typically below 10⁻⁵ mbar.

Measurements of the ion beam energy and current are made using a magnetized retarding field energy analyzer (MRFEA) previously described.⁷ The analyzer has a magnetic filter located at the entrance with a

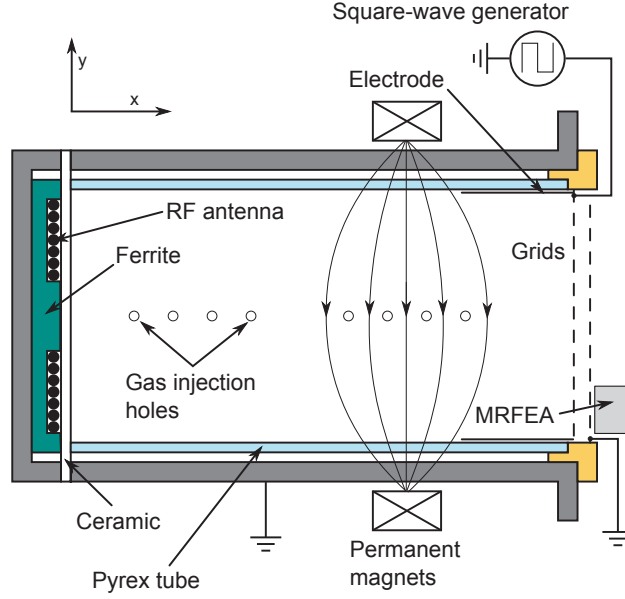


Figure 1. Schematic of the PEGASES plasma source.

strength of about 400 G (which prevents the collection of electrons), a single grounded grid, and a collector plate that can be swept to discriminate the incoming ion energy. A large floating target plate is placed downstream of the PEGASES source, and is used to determine the level of beam plasma neutralization.

III. Experimental results

A. Role of the magnetic filter

Before discussing the alternate ion extraction and acceleration, we briefly clarify the role of the magnetic filter used in the plasma source. Figure 2 shows the measured electron temperature inside, and along the thruster axis, obtained with a Langmuir probe, both with and without the magnetic filter.⁸ Because of the difficulty in measuring the electron temperature in an almost electron-free ion-ion plasma,¹¹ the results in Fig. 2 have been performed in argon (hence no negative ions are present).

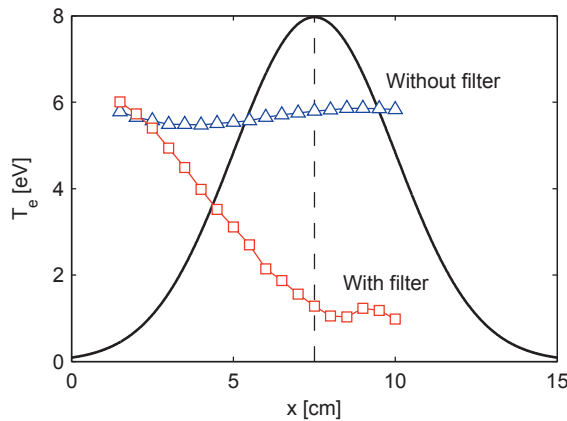


Figure 2. Electron temperature along the axis of the plasma source without (open triangles) and with (open squares) the magnetic filter. The black solid line shows the relative amplitude of the axial magnetic field profile.

As seen in Fig. 2, with no magnetic filter the electron temperature remains almost constant along

the length of the source and has an average value of about 6 eV. However, when the magnetic filter is present the electron temperature is observed to rapidly decrease across the filter, going from 6 eV in the upstream region near the antenna, down to less than 1 eV in the region near the source exit. Thus the role of the magnetic filter is to reduce the electron temperature by significantly lowering the electron thermal conductivity. This reduced electron temperature (and hence average energy) facilitates the formation of negative ions (in electronegative gases) by attachment, and with SF₆, the result is that the electronegativity of the plasma downstream of the filter is of the order of a 1000. Previous probe measurements^{7,11} have also shown that in this region the positive and negative ion densities are about $1 \times 10^{17} \text{ m}^{-3}$, the ion temperatures are 0.1 eV, and the current density to the grids is about 1 mA/cm².

B. Ion acceleration

For the ion acceleration tests, we use a combination of argon and SF₆ in a flow rate ratio of 50-50 (13 SCCM = 0.39 mg/s for argon, and 13 SCCM = 1.34 mg/s for SF₆). This is because it is difficult to ignite a pure SF₆ plasma, and previous results have indicated that the electronegativity near the grids does not change much for higher percentages of SF₆. For all results presented below the total power supplied from the rf power generator is 200 W, and due to losses in the transmission line and the matching network, the total power absorbed by the plasma is about 100 W. At the flow rates specified above, the pressure inside the plasma source is about 1 mTorr, while the downstream vacuum chamber pressure is about 0.1 mTorr.

Because the walls of the thruster are insulating, the only potential reference that the plasma is in direct contact with is the first grid. Thus the plasma potential will follow the applied voltage to this grid. By applying square voltage waveforms to the grids with different voltage amplitudes, frequencies, and duty cycles, the ion extraction and acceleration is measured with the MRFEA, which is located just after the grids. Figure 3 (a) shows an example of a measured ion distribution function (IF-DF) obtained at 200 kHz, a duty cycle of 50%, and a voltage amplitude of 350 V. As can be seen, there are three distinct peaks: (1) a large positive peak centered at about 350 V which represents accelerated positive ions, (2) a slightly smaller peak centered at about -350 V and which represents accelerated negative ions, and (3) a small central peak which is an artefact of the probe (i.e. secondary electron emission from the probe, and/or the surface productions of low energy negative ions). Figure 3 (b) shows the measured positive and negative ion beam energies as a function of the applied square waveform frequency. As can be seen, over the whole range of tested frequencies, the positive and negative ion energies are almost constant and have no strong frequency dependence. The negative ion energy is slightly lower by about 5 – 10%. This behaviour is not fully understood, but is thought to be related to the presence of residual electrons near the extraction grids. The measured IF-DF in Fig. 3 were made with a probe located close to the grids. By instead moving the probe 10 cm away, the relevant ion beams can still be easily discerned (not shown).

It is difficult to accurately measure the mass composition of the extracted ions at present, although fluid simulations¹² suggest that the dominant positive ion is expected to be SF₅⁺, while the dominant negative ions are SF₆⁻ and F⁻. Langmuir probe measurements using the model in Ref.¹¹ have found a good fit to measured *IV* curves for an ion mass of 127 AMU, which is consistent with SF₅⁺ or SF₆⁻ ions.

C. Positive and negative ion current extraction

Figure 4 (a) shows the time-averaged positive and negative ion current densities extracted from the thruster as a function of the square waveform frequency for a voltage amplitude of 350 V, and a duty cycle of 50%. The ion beam current here has been defined as the 1- σ width of the Gaussian shaped beams seen in the IF-DFs (see Fig. 3 (a)). As can be observed, as the applied frequency increases, the extracted current decreases, until a value of about 40% lower is reached at a frequency of 850 kHz. For further increases in frequency the ion current begins to increase again. The extracted current densities are relatively low for the present prototype, because the voltage amplitude and the distance between the grids results in a space-charge limited current density lower than the Bohm-type current directed towards the first grid from the plasma in the source.

It is clear from Fig. 4 (a) that at a duty cycle of 50%, the positive ion current density extracted is almost twice as large as the negative ion current extracted. This can occur because of the presence of co-extracted electrons, radial non-uniformities, or because of different positive and negative ion masses. It is important though that a mechanism exists to be able to control the level of current extraction in order to prevent charging of the thruster/spacecraft. Figure 4 (b) shows the extracted currents as a function of duty cycle

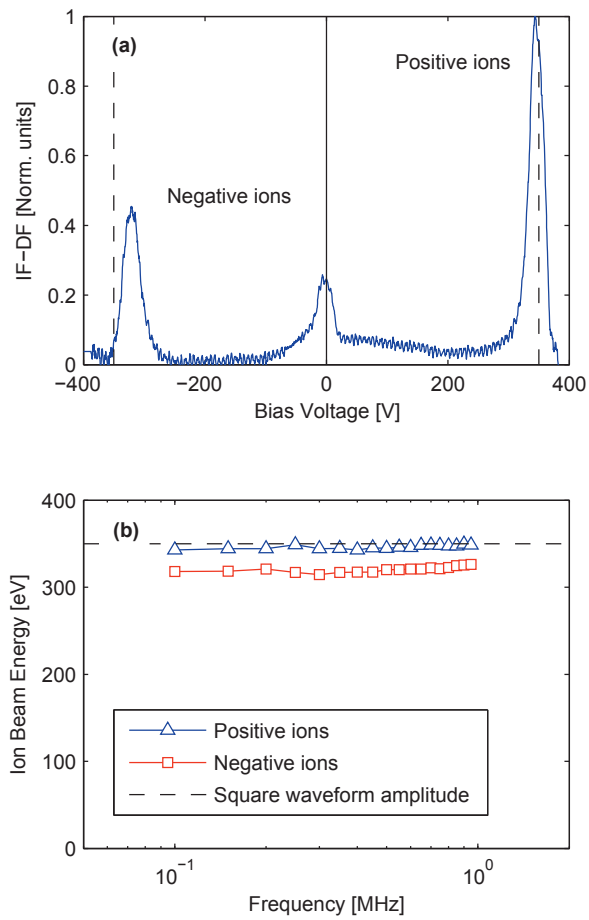


Figure 3. (a) Normalized ion distribution function measured with the MRFEA for an applied square waveform frequency of 200 kHz. (b) Ion energies as a function of the applied square waveform frequency. The voltage amplitude is 350 V and the duty cycle is 50%.

for a frequency of 200 kHz. As seen, when the duty cycle is changed, the positive and negative ion beam currents can be controlled. In particular, at a duty cycle of about 35% the positive and negative ion beam currents are equal. Thus a mechanism exists to control the oppositely charged particle extraction and to prevent spacecraft charging.

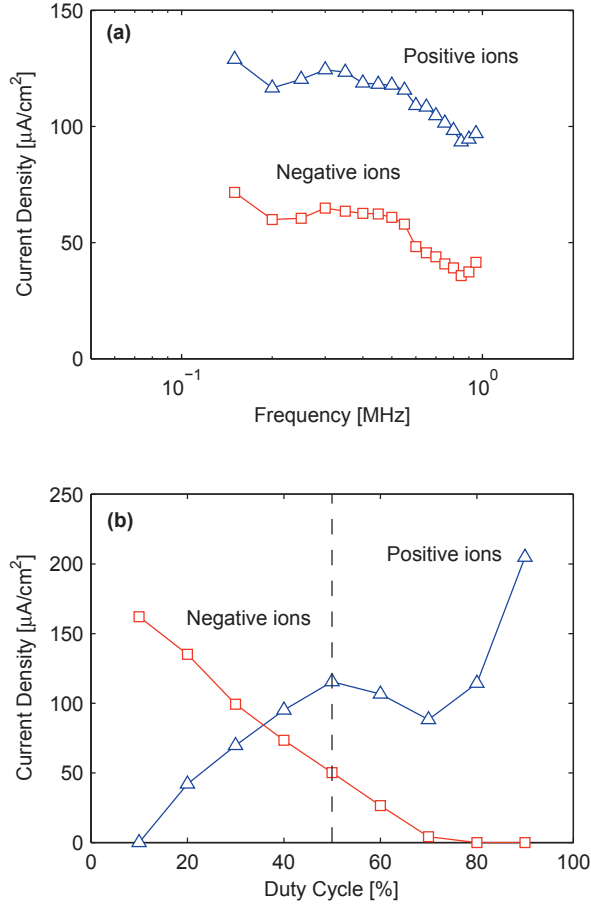


Figure 4. (a) Extracted current densities as a function of the applied square waveform frequency for a voltage amplitude of 350 V and a duty cycle of 50%. (b) Extracted current densities as a function of the square waveform duty cycle for an applied frequency of 200 kHz.

D. Beam neutralization

Although we have shown that positive and negative ions can be extracted and accelerated, it is important to know whether the beam charge can be neutralized in the downstream region. Using the floating target plate placed in the plume, the temporal variation of the floating potential is measured, and compared with the square voltage waveform applied to the grids. Previous measurements⁶ have indicated the presence of co-extracted electrons in the downstream which can assist in the neutralization process. These electrons are present because of an $\mathbf{E} \times \mathbf{B}$ drift^{13,14} on one side of the thruster (due to the applied filter magnetic field, and the electric field in the sheath/presheath near the side walls of the source) which is directed towards the grids. These co-extracted electrons can be blocked by manually closing off about one third of the grid on the side with the drift.

Figure 5 shows the applied voltage and the floating potential at two extraction frequencies: (a) 20 kHz, and (b) 200 kHz. As seen, at the low frequency the target charges up and floats to almost the same potential as the accelerated positive and negative ions at each of their respective extraction/acceleration cycles. This

indicates that the downstream plume is poorly neutralized, and hence that beam stalling and ion reflection will occur, significantly reducing the thruster operation. By contrast, at the larger frequency the floating potential of the target is just a few 10's of volts during both positive and negative cycles, which indicates good beam space charge neutralization; either because the alternate beam packets have mixed, or because the net charge in each packet is small enough that space charge effects are minimized.

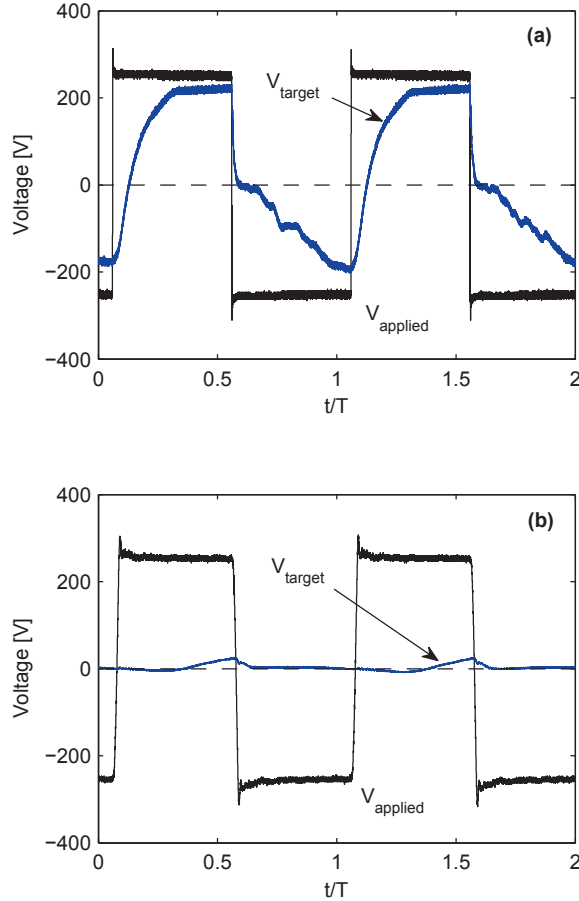


Figure 5. Applied square voltage waveform, $V_{applied}$, and floating potential of the downstream target plate, V_{target} , as a function of time for (a) 20 kHz, and (b) 200 kHz. The voltage amplitude is 250 V and the duty cycle is 50%.

IV. Theoretical results

A. Extension of the Child-Langmuir law

Because of the time-varying square voltage waveforms applied to the PEGASES grids, the extracted ion current densities are no longer expected to follow the scalings of the well-known Child-Langmuir (CL) law. By considering the spatio-temporal charged particle dynamics between the extraction grids, we have been able to generalize⁹ the CL law and obtain expressions for the time-averaged extracted positive and negative ion current densities

$$\frac{J_p^{ac}}{J_p^{dc}} = \alpha - fL\sqrt{\frac{M_p}{q_p V_0}} \quad (1)$$

$$\frac{J_n^{ac}}{J_n^{dc}} = (1 - \alpha) - fL \sqrt{\frac{M_n}{q_n V_0}} \quad (2)$$

where J^{dc} and J^{ac} are the equivalent dc and time-averaged ac extracted current densities, α is the duty cycle, f is the applied frequency, L is the distance between the grids, M and q are the ion mass and charge respectively, V_0 is the square waveform amplitude, and the subscripts p and n refer to positive and negative ions respectively. Equations 1 and 2 are valid for $fL \leq 0.45 \sqrt{\frac{qV_0}{2M}}$. If the grids are operated in a dc mode at conditions that would otherwise be equal to the space-charge limit, then J^{dc} is given by the CL law

$$J^{dc} = J^{CL} = \frac{4\epsilon_0}{9} \sqrt{\frac{2q}{M}} \frac{V_0^{3/2}}{L^2} \quad (3)$$

Here ϵ_0 is the permittivity of free space. Hence Eqns. 1 and 2 would represent the square voltage waveform generalization of the CL law.

B. Verification with particle-in-cell simulations

Ion extraction and acceleration between the grids with square voltage waveforms have also been tested using 1D particle-in-cell (PIC) simulations (see Ref.⁹ for more detailed information). Figure 6 shows the relative extracted current densities for equal mass positive and negative ions as a function of applied frequency for different grid gaps. As seen, the current density decreases until a minimum point is reached, after which the current density increases again. This is in good agreement with the experimental results obtained in Section III C above. The location of the minimum points in the curves in Fig. 6 are found to almost exactly match the frequency where the ion transit time across the grids is equal to one half of the period. This behaviour for the current density is easily understood from the analytical results: when the waveform polarity changes there is a small transient time needed for the ions to cross the gap between the grids, and hence for the full current level to be established. As the frequency increases though, this transit time starts to become a more and more significant portion of the rf period, and thus the time portion during which the full current level is extracted decreases. Eventually, as the frequency increases further, the ions can no longer respond to the time-varying electric field because of their large inertia, and for sufficiently large frequencies, they will simply drift out completely unimpeded.

The scaling laws identified in Eqns. 1 and 2 have been tested by running simulations with different ion masses, applied frequencies, grid gaps, and voltage amplitudes. The measured current is then compared with that given by Eqns. 1 and 2. As seen in Fig. 6 (b), the results (which include almost 80-90 simulations in total) are in excellent agreement, and almost exactly lie on the expected theoretical curve.

C. Control of the positive and negative ion beam currents

By changing the mass of the positive and negative ions, it is interesting to confirm the experimental result obtained in Section III D that the extracted currents can be controlled by adjusting the duty cycle. This is shown in Fig. 7 for negative ions with a mass 10 times lower than the positive ions. The data points show PIC simulation results, while the lines show the results from Eqns. 1 and 2. As seen, at a duty cycle of 50% the extracted currents are not equal. However, for a duty cycle of about 60% equal positive and negative ion current densities can be extracted. This is in good qualitative agreement with the experimental results.

V. Conclusions

In summary, we have experimentally demonstrated the working principles of the PEGASES plasma thruster, which alternatively extracts and accelerates positive and negative ions to generate thrust. No separate electron hollow cathode neutralizer is needed, and we have shown that high energy ions can be produced and that good beam neutralization can be achieved at sufficiently high frequencies (~ 200 kHz). We have also shown that the level of current extraction, and hence spacecraft charging, can be controlled by adjusting the duty cycle of the square voltage waveform applied to the grids. Development work is currently under way to optimize the performance¹⁵ of the system.

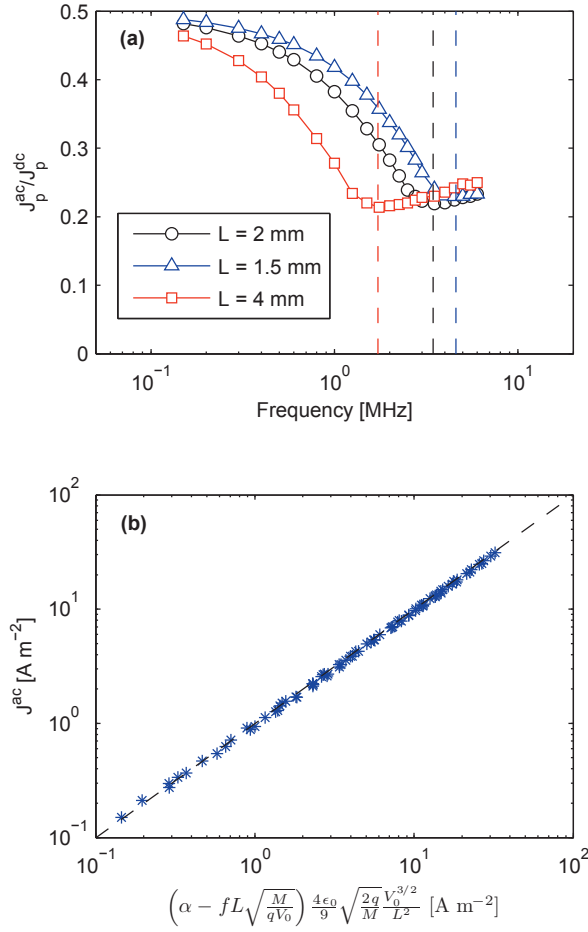


Figure 6. (a) Normalized extracted ion current densities from a 1D PIC simulation as a function of the applied square waveform frequency for different grid gaps. The voltage amplitude is 500 V and the duty cycle is 50%. (b) Time-averaged space-charge limited extracted current densities from a 1D PIC simulation as a function of the combination of Eqns. 1 and 3. The vertical dashed lines in (a) mark the frequency when the ion transit time across the grid gap is equal to one half of the period.

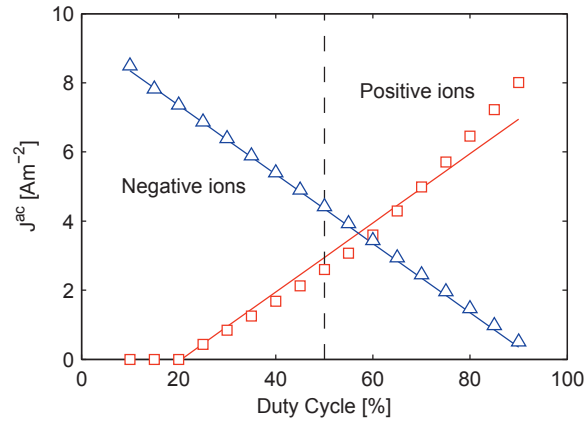


Figure 7. Time-averaged current densities from a 1D PIC simulation as a function of the duty cycle. The solid lines show the theoretical results from Eqns. 1 and 2. The voltage amplitude is 500 V, the grid gap is 2 mm, and the applied frequency is 2 MHz.

Acknowledgments

This work received financial state aid managed by the Agence Nationale de la Recherche as part of the program “blanc” under the reference ANR-2011-BS09-40 (EPIC), the program “Investissements d’avenir” under the reference ANR-11- IDEX-0004-02 (Plas@Par), and by a Marie Curie International Incoming Fellowship within the 7th European Community Framework (NEPTUNE PIIF-GA-2012-326054).

References

- ¹D.M. Goebel and I. Katz, “Fundamentals of Electric Propulsion: Ion and Hall Thrusters”, Wiley, New Jersey, 2008.
- ²E. Stuhlinger, “Ion propulsion for space flight”, McGraw-Hill, New York, 1964.
- ³H. Koizumi and H. Kunitaka, “Performance of the miniature and low power microwave discharge ion engine $\mu 1$ ” *46th AIAA/ASME/SAE/ASEE Joint Propulsion Conference & Exhibit*, Nashville, Tennessee, 25-28 July 2010.
- ⁴M. Ruiz, I. Urdampilleta, C. Bombardelli, E. Ahedo, M. Merino, and F. Cichocki, “The FP7 LEOSWEEP Project: Improving Low Earth Orbit Security With Enhanced Electric Propulsion”, *Space Propulsion Conference*, Cologne, Germany, 19-22 May 2014.
- ⁵A. Aanesland, A. Meige, and P. Chabert, “Electric propulsion using ion-ion plasmas”, *J. Phys.: Conf. Ser.*, **162**, 012009, 2009.
- ⁶T. Lafleur, D. Rafalskyi, and A. Aanesland, “Alternate extraction and acceleration of positive and negative ions from a gridded plasma source”, *Plasma Sources Sci. Technol.*, **24**, 015005, 2015.
- ⁷D. Rafalskyi, L. Popelier, and A. Aanesland, “Experimental validation of the dual positive and negative ion beam acceleration in the plasma propulsion with electronegative gases thruster”, *J. Appl. Phys.*, **115**, 053301, 2014.
- ⁸T. Lafleur and A. Aanesland, “Ambipolar and non-ambipolar diffusion in an rf plasma source containing a magnetic filter”, *Phys. Plasmas*, **21**, 063510, 2014.
- ⁹T. Lafleur and A. Aanesland, “Generalization of the Child-Langmuir law to the alternate extraction of positive and negative ions”, *Phys. Plasmas*, **21**, 123506, 2015.
- ¹⁰M. Bacal, J. Bruneteau, and P. Devynck, “Method for extracting volume produced negative ions”, *Rev. Sci. Instrum.*, **59**, 2152, 1988.
- ¹¹J. Bredin, P. Chabert, and A. Aanesland, “Langmuir probe analysis of highly electronegative plasmas”, *Appl. Phys. Lett.*, **102**, 154107, 2013.
- ¹²D. Levko, L. Garrigues, and G.J.M. Hagelaar, “Chemical composition of SF6 low-pressure plasma in magnetic field”, *J. Phys. D: Appl. Phys.*, **47**, 045205, 2014.
- ¹³St. Kolev, G.J.M. Hagelaar, G. Fubiani, and J.P. Boeuf, “Physics of a magnetic barrier in low-temperature bounded plasmas: insight from particle-in-cell simulations”, *Plasma Sources Sci. Technol.*, **21**, 025002, 2011.
- ¹⁴J.P. Boeuf, J. Claustre, B. Chaudhury, and G. Fubiani, “Physics of a magnetic filter for negative ion sources. II. $\mathbf{E} \times \mathbf{B}$ drift through the filter in a real geometry”, *Phys. Plasmas*, **19**, 113510, 2012.
- ¹⁵A. Aanesland, D. Rafalskyi, T. Lafleur, P. Grondein, P. Chabert, S. Mazouffre, D. Renaud, L. Garrigues, G.J.M. Hagelaar, and D. Levko, “Development and test of the negative and positive ion thruster PEGASES” *50th AIAA/ASME/SAE/ASEE Joint Propulsion Conference & Exhibit*, Cleveland, Ohio, 28-30 July 2014.